Meccanica (2008) 43: 339–348
DOI 10.1007/s11012-007-9098-y

# Detection of rolling bearing defects using discrete wavelet analysis

**Abderrazek Djebala · Nouredine Ouelaa · Nacer Hamzaoui**

Received: 15 May 2006 / Accepted: 24 September 2007 / Published online: 29 November 2007


**Abstract** In the detection of bearing faults the so much desired objective remains the extraction of the defect vibratory signature from the measured signal in which immerses the random noise and other components of the machine. In this article a denoising method of the measured signals is presented. Based on the optimization of wavelet multiresolution analysis, it uses the kurtosis as an optimization and evaluation criterion, several parameters were then selected. The experimental results show the validity of this method within the detection of several defects simulated on ball bearings. The various configurations, in which the signals were measured, allow leading to optimum conditions of its application. The application of WMRA on filtered signals allows better results than its application on wide bands signals or a simple band pass filtering.

**Keywords** Shocks signals · Wavelet multiresolution analysis · Kurtosis · Defect detection · Mechanics of machines

A. Djebala (✉) · N. Ouelaa
Laboratory of Mechanics and Structures, University of Guelma, P.B. 401 24000 Guelma, Algeria
e-mail: djebala_abderrazek@yahoo.fr

N. Hamzaoui
Laboratory of Vibration-Acoustics, INSA of Lyon, Bâtiment A. de St. Exupéry, 25 bis Avenue Jean Capelle, 69621 Villeurbanne cedex, France

## 1 Introduction

Currently, vibratory analysis became the most reliable tool for the conditional maintenance of rotating machines. The associated techniques evolved so much that one passed from a simple late detection to the diagnosis, even the prediction. Researches in this field are directed towards the possibility of an early detection, several signal processing techniques, often adapted to a precise defect type, were established throughout these last years [1].

Rolling bearings are the principal components of rotating machine. They are often subjected to various excitations which can cause dangerous accidents. For this reason majority of the vibratory analysis applications are on the possibility of an early detection of these elements.

In time domain kurtosis and crest factor proved their efficiency as a reliable indicators of the bearings degradation state. Indeed with each passage of the ball or rolling element on the defect, periodical impacts will be generated. These impacts modify the signal amplitudes distribution, the kurtosis and the crest factor being very sensitive to the shape of the signal, will detect the presence of these impacts and consequently the defect. A kurtosis higher than three and a crest factor higher than six is sign of shocks. In several works the kurtosis was shown more sensitive than the crest factor. Based on the work of the famous British mathematician Pearson, it saw its first application on the bearings by Dyer [2]. The kurtosis is very sensitive to the rotation speed and the frequency bandwidth, it finds its efficiency in narrow bands at high frequencies especially for incipient defects [3, 4]. Compared with other statistical indicators, it proved its superiority in the vibro-acoustic analysis of signals induced by defective bearings [5].

Unfortunately, because of the mask effects, its reliability is immediately limited. Indeed, the noise and other components of the machine will pollute the signal making the impacts invisible, in this condition the detection is difficult, even impossible for incipient defects. A first solution consists in filtering the signal to extract only the defect signature. The high frequency resonance technique, based on the work of MacFadden [6], is undoubtedly the most famous method which proved its efficiency throughout these last years. Still called envelope method it consists to demodulate the signal by a band pass filtering around one of the system structural resonances and then to apply the Hilbert transform and the inverse Fourier transform.

These last years, several techniques were also applied to signals measured on defective bearings. The adaptive filtering, initially conceived by Chaturvedi [7], taken again by several other authors [8], denoising by spectral subtraction [9–11], wavelet denoising [12, 13] and mixture denoising [14].

The wavelet analysis, which appears as the legitimate successor of the famous Fourier transform, was used in several applications as a powerful tool of the bearings defects detection, in continues version in [15–20], or discrete, still called multiresolution analysis, in [21–25]. The last one consists to double filtering the signal by a filter bank called wavelet. It allows a clear visualization of each part of the signal with a resolution adapted to its scale. Wavelet analysis was also applied by several researchers for the gears defects detection in [26–29].

Actually in several works, the application of wavelet multiresolution analysis is carried out without a rational choice of the analysis parameters what influences the result obtained inevitably. The contribution of this work is to adapt the WMRA to the detection of defects inducing periodical impulsive forces by the choice and the optimization of several parameters using the kurtosis as principal criterion. Associated to envelope and spectral analyses it allows clear visualization of the characteristic frequencies of different bearings defects.

## 2 Mask effect and its influence on the defect detection

Figure 1 represents a simulated impulse train, each impulse is modulated by a single harmonic frequency with exponential decay. The signal can be considered as a model of a rolling element bearing defect signature [3, 4]. The defect frequency is taken equal to 100 Hz and the natural frequency to 2800 Hz. The signal is simulated with a frequency bandwidth of [0–15000] Hz. After adding a significant level of white Gaussian noise and two discrete components to simulate low frequencies (60 and 130 Hz), the impulses are completely masked and the detection is not obvious (Fig. 2). The kurtosis decreases from 27.74 for the impulse original signal to 3.34 for the noisy signal.

This simulation shows the influence of the mask effects on the defect detection. Indeed, Fig. 3 shows that the kurtosis decreases considerably with the reduction of the SNR (Signal to Noise Ratio). Dice a frequency

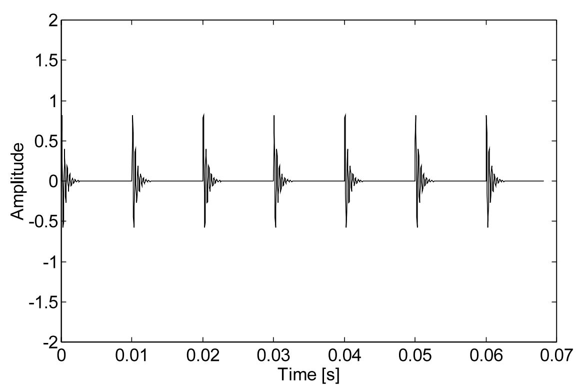


**Fig. 1** Impulse train signal simulating bearing defect at 100 Hz

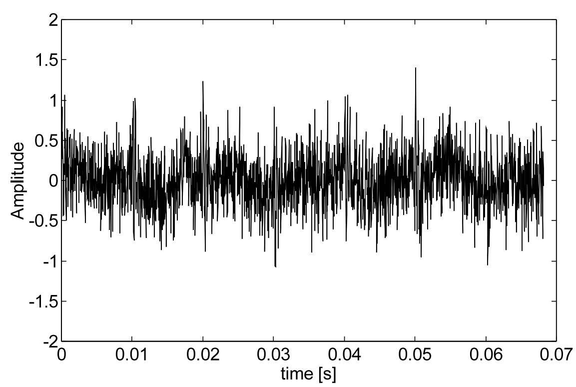


**Fig. 2** Noisy signal

is added to the signal and starting from a certain number of frequencies the detection is not possible for any noise level. Indeed the discrete frequencies, which can model in practice other components of the machine, have as much influence as the background noise.

## 3 Optimization of wavelet multiresolution analysis

### 3.1 WMRA theory

The Discrete Wavelet Transform (DWT), still called Wavelet Multiresolution Analysis (WMRA), consists to introduce a signal $s(t)$ in low-pass ($L$) and high-pass ($H$) filters. In this level, two vectors will be obtained, $cA_1$ and $cD_1$. The elements of the vector $cA_1$ are called *approximation coefficients*, they correspond to the low frequencies of the signal, while the elements of the vector $cD_1$ are called *detail coefficients* and they correspond to the highest of them. The procedure can be repeated with the elements of the vector $cA_1$ and successively with each new vector $cA_j$ obtained. The process of decomposition can be repeated $n$ times, with $n$ the number of levels. Figure 4 represents an example of waterfall decomposition for $n = 3$.

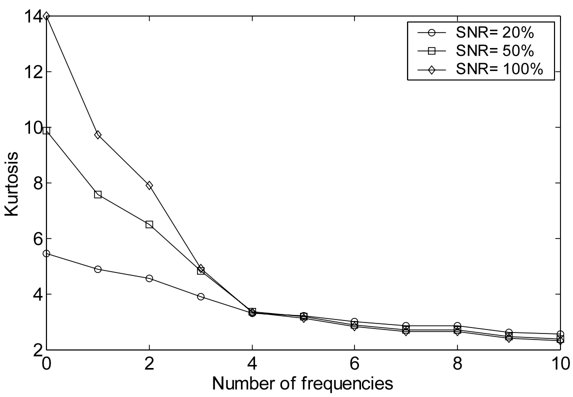


**Fig. 3** Kurtosis in function of frequencies number for different SNR

During the decomposition, the signal $s(t)$ and vectors $cA_j$ undergo a downsampling, this is why the approximation $cA_j$ and detail $cD_j$ coefficients pass through two new reconstruction filters (*LR*) and (*HR*). Two vectors result; $A_j$ called *approximations* and $D_j$ called *details*, satisfying the relation:

$$A_{j-1} = A_j + D_j,$$
$$s = A_j + \sum_{i \le j}^{n} D_i, \qquad (1)$$

where $i$ and $j$ are integers.

### 3.2 Optimal choice of the WMRA levels number

Usually, a bearing defect is detected by its characteristic frequency and some of its harmonics. According to [22], three are sufficient. The frequency bandwidth of the final level $n$ approximation must then contain the shock frequency and three of its harmonics, it must thus satisfy:

$$F_{\max}(A_n) = \frac{F_{\max}(s)}{2^n} = 3F_c. \qquad (2)$$

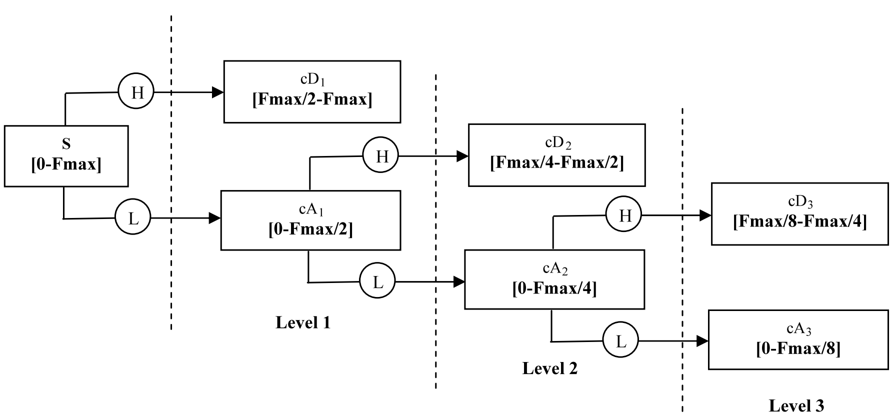


**Fig. 4** Example of waterfall decomposition at three levels

Therefore, the number of levels must, in its turn, satisfy:

$$n = 1.44 \log\left(\frac{F_{\max}(s)}{F_c}\right). \tag{3}$$

with $F_{\max}(A_n)$, $F_{\max}(S)$ and $F_c$ represent the maximum frequency of the final approximation, the signal maximum frequency and the shock (or defect) frequency, respectively.

### 3.3 Choice of the maximum frequency of the signal and the decomposition optimal vector

It is known that a filtering is optimal if the bandwidth of the filter is around the system resonance frequency. Indeed according to [6], in presence of defect, the resonance will be modulated by its characteristic frequency. That means that the frequency bandwidth of the wavelet decomposition optimal vector included the resonance frequency inevitably. Moreover, it's easy to prove that its kurtosis is higher than the other decomposition vectors (other details and approximations). This vector (optimal detail) is called reconstructed signal.

During the decomposition a problem can be posed; it is that the resonance can be cut by the frequential bandwidth of a detail or of an approximation and in this case filtering is not carried out around it. Figure 5

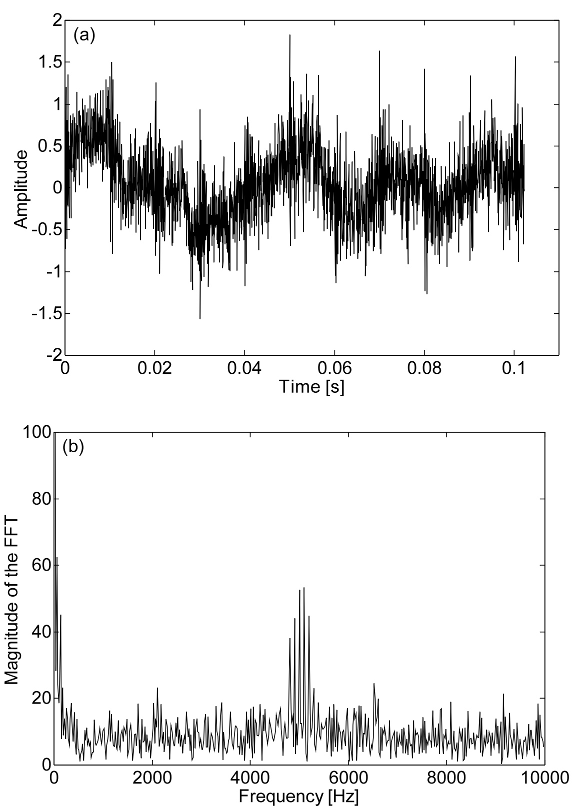


**Fig. 5** **a** Simulated impulses noised signal and **b** Its spectrum [0–10000] Hz, with a natural frequency of 5000 Hz

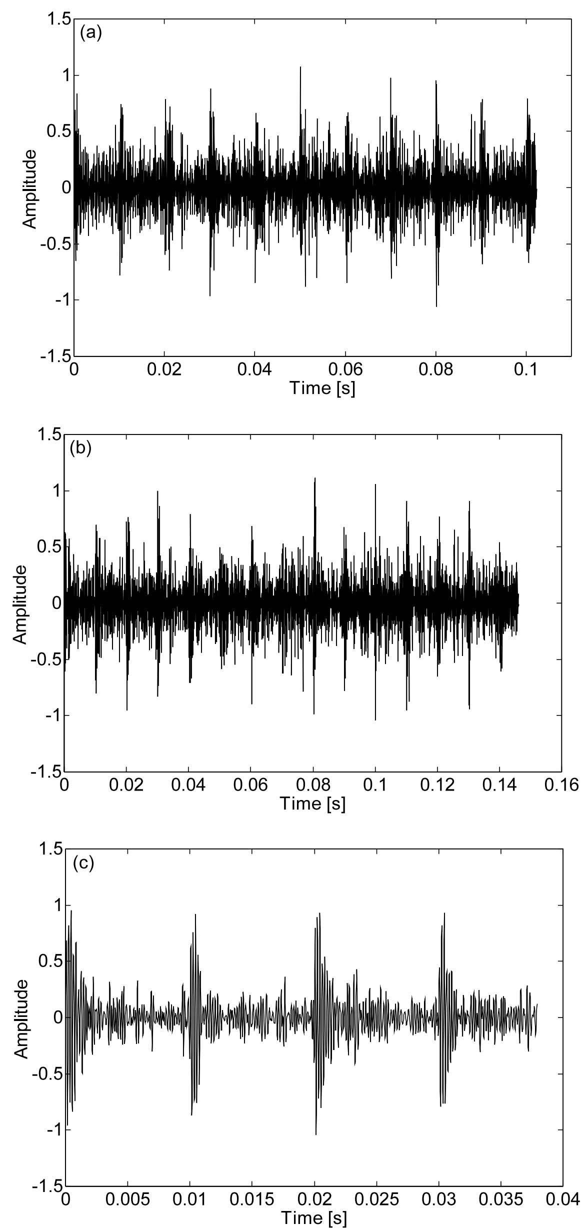


**Fig. 6** Reconstructed signals for a maximum frequency of: **a** 10000 Hz, **b** 7000 Hz and **c** 27000 Hz

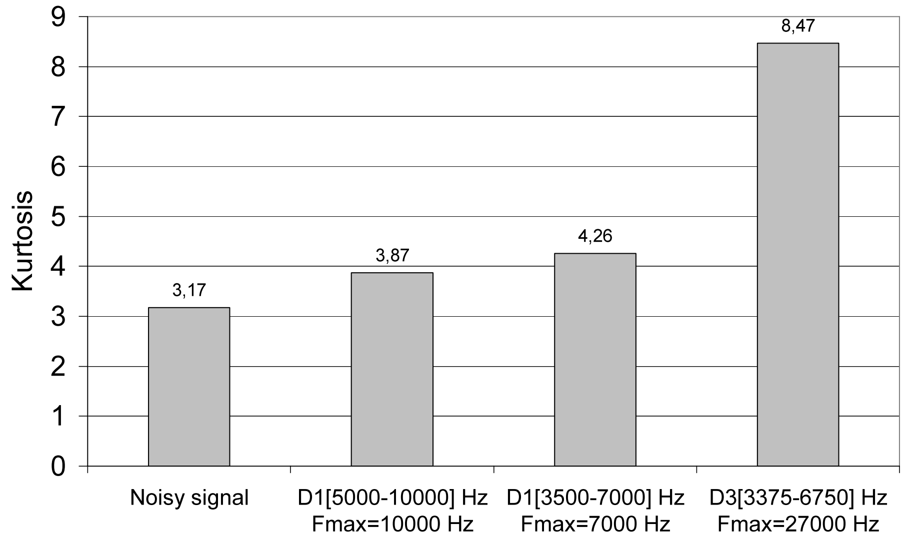


**Fig. 7** Kurtosis of the reconstructed signals in all the considered cases

shows a simulated noised signal and its spectrum with a natural frequency of 5000 Hz, the frequency bandwidth is assumed to be [0–10000] Hz. By applying the Wavelet Multiresolution Analysis the bandwidth of the first detail (D1) must be [5000–10000] Hz, and [0–5000] Hz for the first approximation (A1), so they do not cover the resonance frequency, this is a serious problem.

The solution consists in choosing the maximum frequency of the signal in such a way that at least one or more details will be pass band around the system principal resonance, which one can easily know by the application of WMRA on a signal sufficiently wide band or simply from the wide band spectrum.

Knowing that the bandwidth of each detail (i) is: $[\frac{F_{\max}(s)}{2^i} - \frac{F_{\max}(s)}{2^{i-1}}]$, the resonance frequency $F_r$ must be included in this band, so it must be equal to:

$$F_r = \frac{\frac{F_{\max}(s)}{2^i} + \frac{F_{\max}(s)}{2^{i-1}}}{2}. \tag{4}$$

It is then easy to prove that the maximum frequency of the signal must be equal to:

$$F_{\max}(s) = F_r \frac{2^{i+1}}{3} \tag{5}$$

According to (5), for the previous example, the maximum frequency can be taken equal to 7000 Hz, the bandwidth of the first detail (D1) is then [3500–7000] Hz which cover the resonance frequency (5000 Hz). The optimal case is to take the maximum frequency as high as possible as showed in Sect. 3.4, it can be possible then to take it equal to 27000 Hz approximately, in this case the resonance frequency is covered by the bandwidth of the detail 3 (D3) [3375–6750] Hz. Figure 6 shows the reconstructed (filtered) signals for the previous examples.

Two points can be noted:

1. All the reconstructed signals (details) are more filtered than the noisy signal, the impacts are clearly shown especially for the bandwidth [3375–6750] when taking the highest maximum frequency (27000 Hz);
2. In the last configuration the kurtosis is very significant than in the other cases what confirm the approach developed in this section (see Fig. 7).

### 3.4 Optimal choice of the sampling rate

Figure 8 shows that the defect detection is obvious in the highest sampling rate associated to the smallest shock frequency (or rotation speed in practice), were the kurtosis of the reconstructed signal is significant. Indeed, for low shock frequencies the impacts repetition period is large and the kurtosis is then more significant, studies showed that its optimal capacities are reached if this repetition is bigger than 3 times the relaxation time [3, 4]. On the other hand if the shock frequency is great, so that the condition below is not satisfied or the relaxation time exceeds the impact repetition period, the kurtosis loses all its reliability and its values are almost the same and not significant even for highest sampling rates. In practice, it is then optimal to take the rotation speed as low as possible, if this is not always obvious, the maximal sampling rate is then recommended.

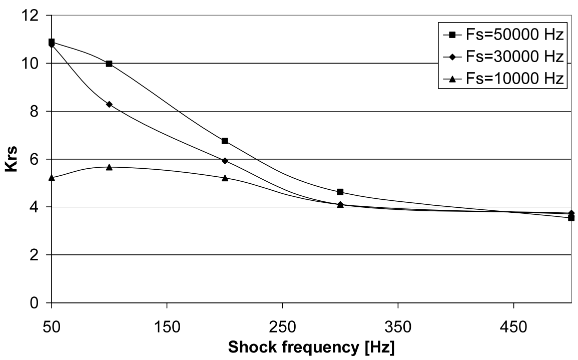


**Fig. 8** Kurtosis of reconstructed signal for different shock and sampling frequencies

### 3.5 Optimal choice of the analysis wavelet

The wavelets are comparable to a band pass-filter. In the present case, the selected wavelet will be that which allows better filtering of the original signal thus a maximum kurtosis of the reconstructed signal. After the elimination of the unsuited wavelets to the WMRA and after computing the kurtosis of the reconstructed signals, maximal values were taken and Table 1 gives the wavelets adapted for each sampling rate and shock frequency (or the ratio $F_s/F_c$).

## 4 Experiments

In order to validate the proposed method, several experiments were carried out on a test rig (see Fig. 9).

**Table 1** Type of wavelets adapted for each configuration

| Sampling rate [Hz] | $F_s/F_c$ | | | | |
|---|---|---|---|---|---|
| | 50 | 100 | 200 | 500 | 1000 |
| 10000 | db5 | db5 | db5 | db5 | db6 |
| 30000 | db5 | db12 | db5 | db6 | db5 |
| 50000 | db6 | db12 | db10 | db5 | db10 |

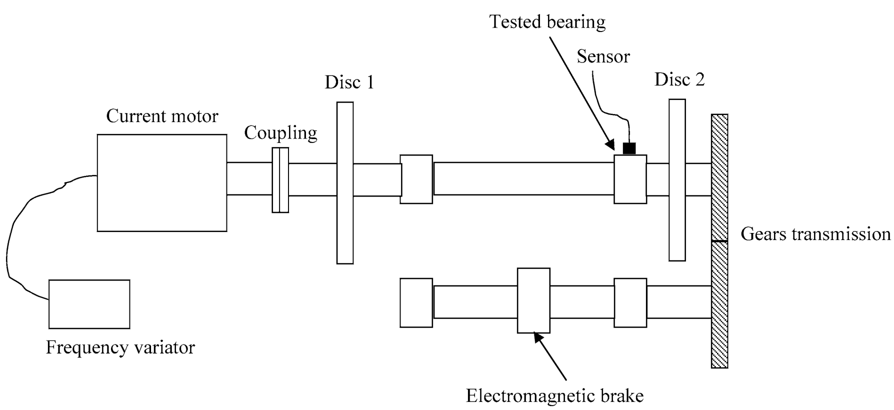


**Fig. 9** Bearings test rig

**Table 2** Details of experiment conditions

| Bearing type | 6200 | | | | | | |
|---|---|---|---|---|---|---|---|
| Bearing No. | 1 | 2 | 3 | 4 | 5 | 6 | 7 |
| Defect type | Outer race | Inner race | Outer race | Inner race | Two on each race | Two on outer race | Ball |
| Defect gravity | Small | Small | Great | Great | Combined | Combined | Small |
| Sampling rates [Hz] | 65536, 32768, 16384, 4096, 1024 | | | | | | |
| Rotation speeds | 50, 30, 15, 10 [Hz] | | | | | | |

Three types of defects were simulated on a 6200 ball bearings, defects were artificially localized in a rectangular shape by a diamante tool turning with 50000 RPM. The defects size are (width × depth) = (1 × 0.3) for the small defect and (1.3 × 0.7) for the great one. Table 2 shows some details concerning the experiments conditions. Measurements were taken by a B&K 4384 type accelerometer and a B&K 2035 type analyzer, the post processing is carried out on Matlab©. The two rotating discs simulate a dynamic load.

The first case examined is that of a 6200 type ball bearing, on which a defect was caused on its outer race, the bearing turns at 50 Hz, in this case the defect characteristic frequency (BPFO) is approximately equal to 131 Hz. Figure 10a shows the signal measured with a sampling rate of 16384 Hz. After the application of the proposed method, the reconstructed signal allows detecting the shocks due to the defect (see Fig. 10b); the envelope spectrum of its wavelet coefficients shows the defect characteristic frequency and some of its harmonics (see Fig. 10c).

In the second case a ball defect was caused, the bearing turns at 30 Hz, the defect characteristic frequency (BDF) is then equal to 56 Hz. Figure 11a shows the signal measured with a sampling rate of 32768 Hz. The reconstructed signal highlights impulses due to the defect (Fig. 11b), its envelope spectrum of the wavelet coefficients clearly shows the frequency component of these impulses and which correspond to a ball defect and some of its harmonics (Fig. 11c).

## 5 Influence of band pass filtering

The signals used until now are measured on a relatively wide frequency bands able to reach 25.6 kHz. The approach developed in this section is to use the WMRA on signals filtered around one of the system resonances. The methodology consists to:

1. Apply the WMRA on a wide band signal and select the reconstructed signal
2. Choose the resonance around which filtering will be applied
3. Apply the WMRA on the filtered signal.

This approach is validated on the signal of Fig. 12a measured on a bearing with an outer race defect, the

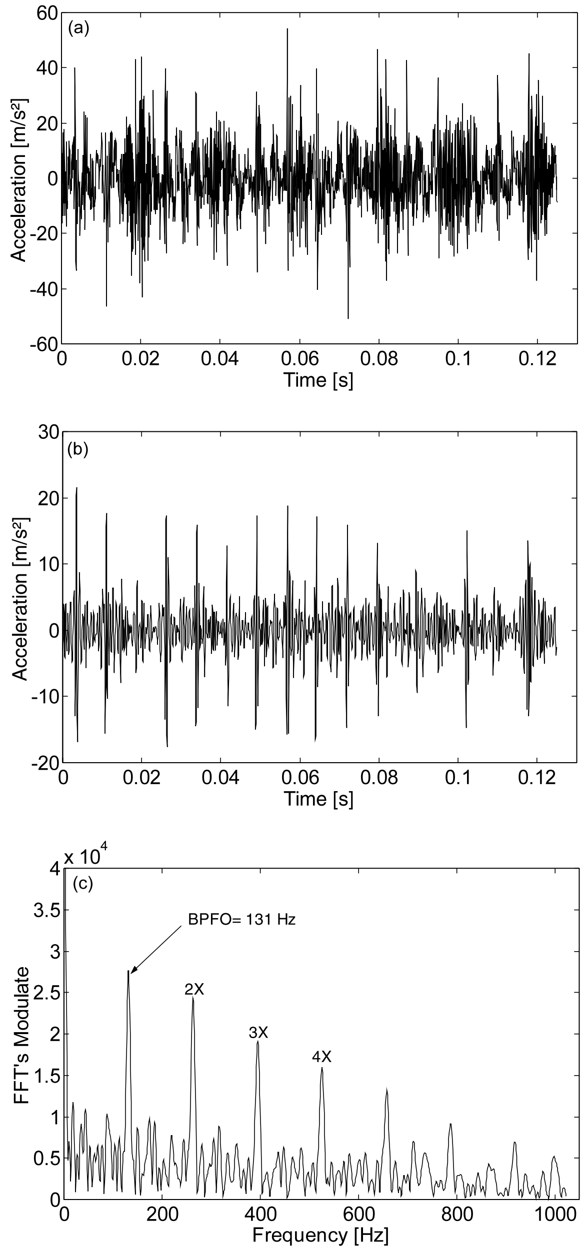


**Fig. 10** **a** Measured signal, **b** Reconstructed signal and **c** Its envelope spectrum of wavelet coefficients. Bearing with outer race defect

frequency bandwidth of this signal is [0–25.6] kHz. The corresponding spectrum highlights resonances equal roughly to 1600, 4000 and 18000 Hz (Fig. 12b). The application of the wavelet multiresolution analysis makes it possible to extract the reconstructed signal from the detail 3 (D3) whose bandwidth is [3200–6400] Hz and which covers actually the second

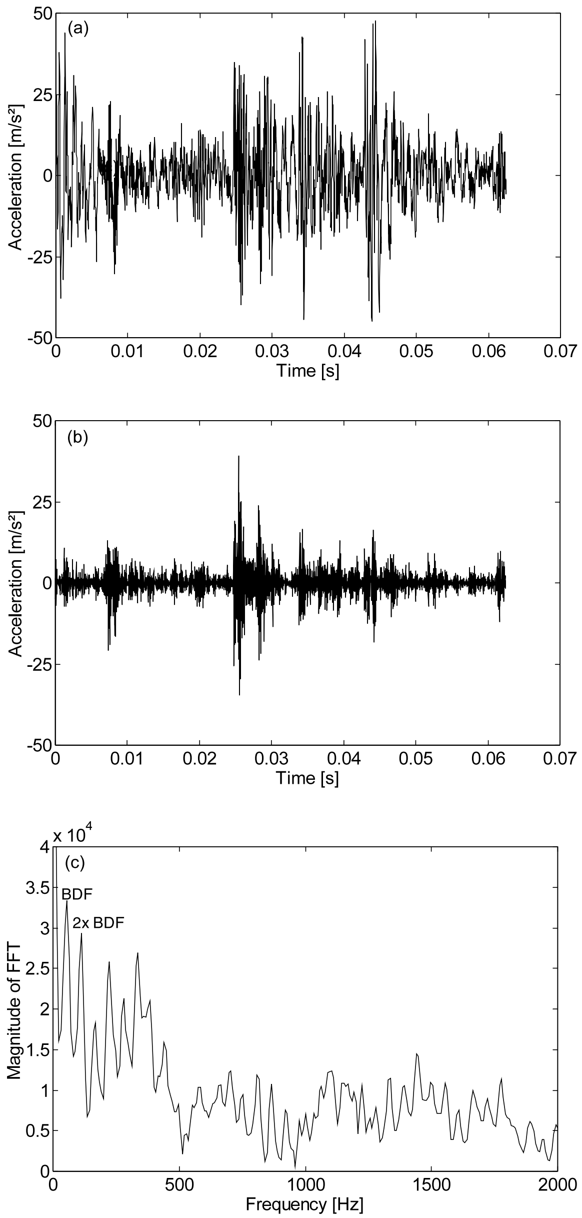


**Fig. 11** **a** Measured signal, **b** Reconstructed signal and **c** Its envelope spectrum of wavelet coefficients. Bearing with ball defect

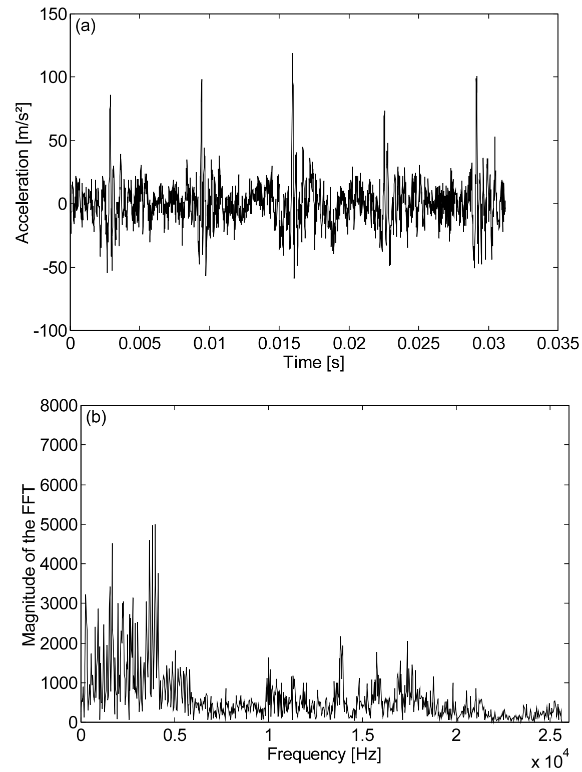


**Fig. 12** **a** Wide band signal measured on defective bearing and **b** Its spectrum [0–25.6 kHz]

resonance frequency (4000 Hz) (Fig. 13a), its kurtosis is higher than other decomposition details and approximation. A band pass filtering of the wide band signal is carried out between 1000 Hz and 5000 Hz (see Fig. 13b). The filtered signal processing by WMRA allows leading to the new reconstructed signal of Fig. 13c. Several other filtering were carried out, each time the filtered signal is treated by the WMRA.

On Fig. 14 one notes that the application of the WMRA on the filtered signal [1000–5000] Hz allows to have maximum kurtosis and consequently optimal filtering compared to other filtered signals processed by the WMRA, this validates the assumption put before. Moreover it is easy to note that even the kurtosis of the reconstructed signal from the wide band signal [0–25.6] kHz is more important than that of the other filtered signals what places wavelet filtering, more optimal in certain cases, than that of a band pass filtering.

Actually this approach seems more consistent in the case of incipient defects, in particular if the detection by a simple band pass filtering or a wide band WMRA is not possible. In conclusion the association of a band pass filtering carefully selected and an optimized WMRA allows to have better result than the application of one of these techniques alone.

## 6 Conclusion

This article presents a denoising method based on wavelet analysis of vibratory signals measured on de-

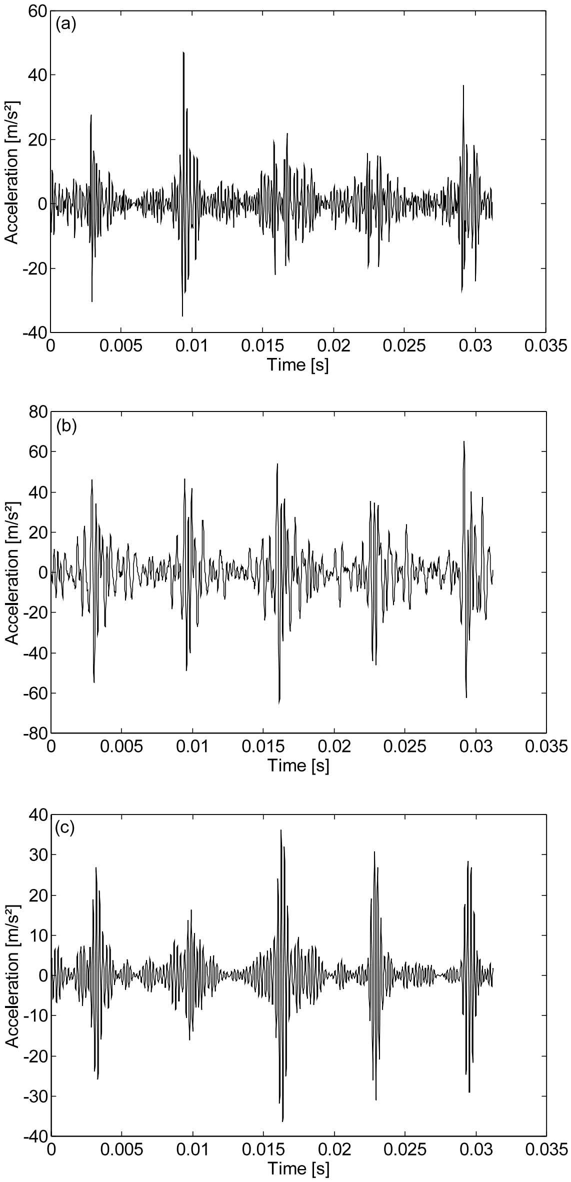


**Fig. 13** **a** Reconstructed signal from the wide band signal, **b** Filtered signal [1000–5000] Hz and **c** Reconstructed signal from the pass band filtered signal

fective bearings. To adapt it to this objective several of the wavelet multiresolution analysis parameters were chosen, even optimized. The kurtosis, being the most sensitive parameter to the shocks, was used as an optimization criterion. After theoretical simulation the method is applied to real signals measured on rolling bearings, on which various defects were simulated. The results obtained show the validity of the method according to the kurtosis values of reconstructed sig-

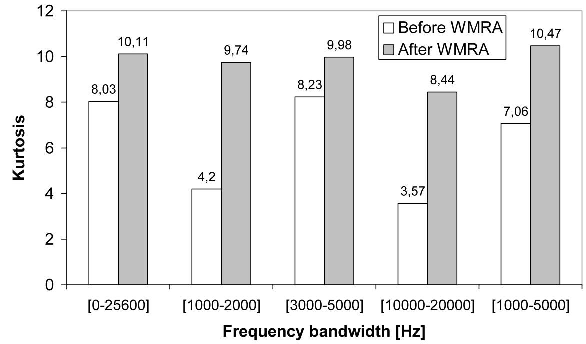


**Fig. 14** Kurtosis of measured and filtered signals before and after the application of WMRA

nals. Moreover, wavelet coefficients envelope spectra allow a clear visualization of the defect characteristic frequency offering the possibility of an early detection. The application of this method proves more interesting on filtered signals. The results show that the WMRA of a signal thoroughly filtered makes it possible to lead to a reconstructed signal whose kurtosis is more important than in the case of a simple band pass filtering or a wide band WMRA. This approach allows an early detection in particular for incipient defects.

## References


1. Tandon N, Choudhury A (1999) A review of vibration and acoustic measurement methods for the detection of defects in rolling element bearings. Tribol Int 32:469–480
2. Dyer D, Stewart M (1978) Detection of rolling element bearing damage by statistical vibration analysis. J Mech Des 100:229–235
3. Boulenger A, Pachaud C (1998) Diagnostic vibratoire en maintenance préventive. Dunod, Paris
4. Pachaud C, Salvetas R, Fray C (1997) Crest factor and kurtosis contributions to identify defects inducing periodical impulsive forces. Mech Syst Signal Process 11(6):903–916
5. Heng RBW, Nor MJ (1998) Statistical analysis of sound and vibration signals for monitoring rolling element bearing condition. Appl Acoust 53(1–3):211–226
6. MacFadden PD, Smith JD (1984) Vibration monitoring of rolling element bearing by the high frequency resonance technique, a review. Tribol Int 17(1):3–10
7. Chaturvedi GK, Thomas DW (1982) Bearings faults detection using adaptive noise cancelling. J Mech Des 104:280–289
8. Khemili I, Chouchane M (2005) Detection of rolling element bearing defects by adaptive filtering. Eur J Mech A: Solids 24:293–303
9. Dron JP, Bolaers F, Rasolofondraibe L (2003) Optimization de la détection des défauts de roulements par débruitage des signaux par soustraction spectrale. Mec Ind 4:213–219

10. Dron JP, Bolaers F, Rasolofondraibe L (2004) Improvement of the sensitivity of the scalar indicators (crest factor and kurtosis) using a de-noising method by spectral subtraction: application to the detection of defects in ball bearings. J Sound Vib 270:61–73
11. Bolaers F, Cousinard O, Marconnet P, Rasolofondraibe L (2004) Advanced detection of rolling bearing spalling from de-noising vibratory signals. Control Eng Pract 12:181–190
12. Donoho DL (1995) De-noising by soft thresholding. IEEE Trans Inf Theory 41(3):613–627
13. Qiu H, Lee J, Lin J, Yu G (2006) Wavelet filter-based weak signature detection method and its application on rolling element bearing prognostics. J Sound Vib 289:1066–1090
14. Shao Y, Nezu K (2004) Design of mixture de-noising for detecting faulty bearing signals. J Sound Vib 282:899–917
15. Lin J (2000) Feature extraction based on Morlet wavelet and its application for mechanical fault diagnosis. J Sound Vib 234(1):35–148
16. Peter W (2000) Wavelets analysis-A flexible and efficient fault diagnostic method for rolling element bearing. In: 7th international congress on sound and vibration, Germany, 4–7 July 2000, pp 507–514
17. Sun Q, Tang Y (2002) Singularity analysis using continuous wavelet transform for bearing fault diagnosis. Mech Syst Signal Process 16(6):1025–1041
18. Rubini R, Meneghetti U (2001) Application of the envelope and wavelet transform analyses for the diagnosis of incipient faults in ball bearings. Mech Syst Signal Process 15(2):287–302
19. Boltezar M, Simonovski I, Furlan M (2003) Faults detection in DC electro motors using the continuous wavelet transform. Meccanica 38:251–264
20. Yang DM, Stronach AF, MacConnell P (2003) The application of advanced signal processing techniques to induction motor bearing condition diagnosis. Meccanica 38:297–308
21. Brabhakar S, Mohanty AR, Sekhar AS (2002) Application of discrete wavelet transform for detection of ball bearings race faults. Tribol Int 35:793–800
22. Nikolaou NG, Antoniadis IA (2002) Rolling element bearing fault diagnosis using wavelet packets. NDT & E Int 35:197–205
23. Mori K, Kasashima N, Yoshioda T, Ueno Y (1996) Prediction of spalling on a ball bearing by applying discrete wavelet transform to vibration signals. Wear 8:195–162
24. Li JC, Jun M (1997) Wavelet decomposition of vibrations for detection of bearing-localized defects. NDT & E Int 30(3):143–149
25. Chinmaya K, Mohanty AR (2006) Monitoring gear vibrations through motor current signature analysis and wavelet transform. Mech Syst Signal Process 20(2):158–187
26. Wang WJ, MacFadden PD (1996) Application of wavelets to gearbox vibration signals for fault detection. J Sound Vib 192(5):927–939
27. Zheng H, Li Z, Chen X (2002) Gear faults diagnosis based on continuous wavelet transform. Mech Syst Signal Process 16(2–3):447–457
28. Yoshida A, Ohue Y, Ishikawa H (2000) Diagnosis of tooth surface failure by wavelet transform of dynamic characteristics. Tribol Int 33:273–279
29. Sung CK, Tai HM, Chen CW (2000) Locating defects of gear system by the technique of wavelet transform. Mech Mach Theory 35:1169–1182